CENBG-R--8601

[illegible] OF [illegible] METHOD[illegible] THE [illegible] SPECTROMETER [illegible]

BETA-DECAY OF LIGHT NEUTRON-RICH EXOTIC NUCLEI

Presented at the XXIV International Winter Meeting

on Nuclear Physics

BORMIO (January 1986)

F. HUBERT

CENTRE D'ETUDES NUCLEAIRES DE BORDEAUX-GRADIGNAN

LE HAUT-VIGNEAU, 33170 GRADIGNAN, France

CENBG - R-- 8601

APPLICATION OF THE PFIS METHOD TO THE LISE SPECTROMETER AT GANIL† : BETA DECAY OF LIGHT NEUTRON RICH EXOTIC NUCLEI

F. HUBERT, J.P. DUFOUR, R. DEL MORAL, H. EMMERMANN,
D. JEAN, C. POINOT, M.S. PRAVIKOFF, A. FLEURY
Centre d'Etudes Nucléaires de Bordeaux-Gradignan
Le Haut Vigneau F-33170 GRADIGNAN
France

H. DELAGRANGE
GANIL - B.P. 5027 F-14021 CAEN Cedex
France

H. GEISSEL, K.-H. SCHMIDT
Gesellschaft für Schwerionenforschung
D-6100 DARMSTADT
Federal Republic of Germany

Abstract :

Radioactive studies of light neutron rich exotic nuclei have been performed on the LISE line at GANIL. These isotopes were produced via projectile nuclear fragmentation of 60 MeV/nucleon ^{40}Ar on Be. Physical separation of the nucleides was achieved through the Projectile Fragment Isotopic Separation (PFIS) method (magnetic analysis and differential stopping power effects). At least 8 nuclei were observed for the first time through β-γ coincidence measurements (^{40}S, ^{38}P, ^{37}P, ^{36}Si, ^{35}Si, ^{24}F, ^{17}C, ^{22}O) as well as already known half-lives to provide a check of the procedure (^{36}P, ^{30}Mg, ^{32}Al).

† Experiment performed at the GANIL National Laboratory in Caen (France)

I - INTRODUCTION

The production and study of exotic nuclei have been continuously investigated since many years from an experimental as well as theoretical point of view. Recently this research field has renewed the interest of experimentalists due to the availability now or in the near future of high intensity heavy ion beams accelerated at intermediate or relativistic energy. The projectile fragmentation mechanism can then be used to produce exotic nuclei with the high rates needed for radioactive studies (1).

This paper reports on theoretical and experimental work showing that the LISE spectrometer at GANIL is well suited for a Projectile Fragment Isotopic Separation (PFIS). The half-life measurements and β-γ spectroscopies of neutron rich light nuclei obtained in the first experiment demonstrate the efficiency of such a method.

In the following, section 2 briefly describes the experimental set-up. The PFIS method and the calculated properties of the LISE line are detailed in section 3. Then the results of an experiment using the nuclear fragmentation of 60 MeV/n ^{40}Ar ions on Be are given in section 4.

II - EXPERIMENTAL SET-UP

The present experiment was performed on the LISE line at GANIL. LISE is a doubly achromatic system, in angle and energy consisting of ten quadrupoles and two dipoles ; a schematic drawing is shown in Fig. 1. Details about the LISE spectrometer can be found in

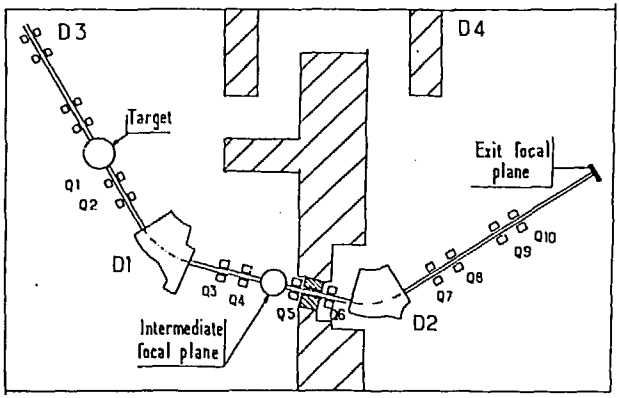

Fig. 1 : Schematic drawing of the LISE spectrometer at GANIL. Q_1 to Q_{10} designate the quadrupoles. D_1 and D_2 designate the dipoles.

Ref. 2. In the focal plane of the first dipole, adjustable slits allow one to limit the magnetic rigidity acceptance of the line. For the PFIS method, an energy degrader made of an aluminium wedge (with a thickness ranging from 200 μ to 1400 μ) was placed behind the slits. The interest of such a procedure is explained in the next section. After transmission through the second dipole the selected projectile fragments entered the counting area (see Fig. 2). These fragments were

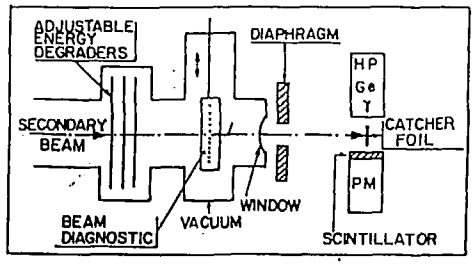

Fig. 2
Sketch of the experimental set-up allowing the range selection and the study of gamma spectroscopy in coincidence with beta decays.

discriminated according to their total ranges in aluminium using a set of Al foils placed 1 m ahead of the detectors. Finally the selected nuclei were stopped in a catcher tape surrounded by a beta plastic scintillator and an ultra pure, high efficiency, high resolution intrinsic germanium gamma detector.

The radioactive nuclei were identified by their γ spectra measured in coincidence with their β decay. Lifetime measurements were carried out using pulsed beam. The length of the beam-off time interval was chosen to be several times the presumed half-life of the studied nuclei. Each event was characterized in time by a clock during beam-on as well as beam off cycles. In order to eliminate the built-up of unwanted long periods, the tape was periodically moved during beam-on cycles.

III - THE PFIS METHOD

III - 1 - Principle of the method

The method used to separate a definite nucleus of atomic charge Z and atomic mass A among the large number of projectile fragments (P.F.) formed in nuclear fragmentation consists in the following steps :

i) the first dipole provides a momentum selection and allows the transmission of a fraction of the produced isotopes. Since the reaction mechanism approximately conserves the velocity, this

selection is mainly sensitive to the ratio $r_1 = A/Z$. Detailed calculations show that the target thickness plays a crucial role to optimize the transmission yields (see section III-3).

ii) after the first dipole the selected ions undergo a slowing down in a thick degrader and lose momentum differentially according to their A and Z. This momentum loss is exploited by the second dipole to provide a second separation inside the subset of nuclei having A/Z constant. This second selection is roughly sensitive to the ratio $r_2 = A^{2.5}/Z^{1.5}$ (see section III-2).

iii) finally at the exit of the second dipole, the selected isotopes are stopped at different depths in aluminium absorbers.

The remarquable feature of these selections characterized by the ratios r_1 and r_2 is that they depend neither on the beam energy and nature nor in the tuning of the line or on the degrader's thickness in the case of experiments performed at GANIL.(energies ranging from 20 to 100 MeV/u). In fig. 3,representing the part of the chart of the nuclides on interest in the present experiment, is shown how these selections work.The ions selected by the first dipole are located on the straight lines corresponding to several A/Z ratios (represented from 1.75 to 3). The ions selected by the second dipole are located on the curves corresponding to several $A^{2.5}/Z^{1.5}$ ratios (represented from 30 to 250). Each selection has a given width in the (N, Z) plane (locally represented by the dotted lines) and the nuclei transmitted by the

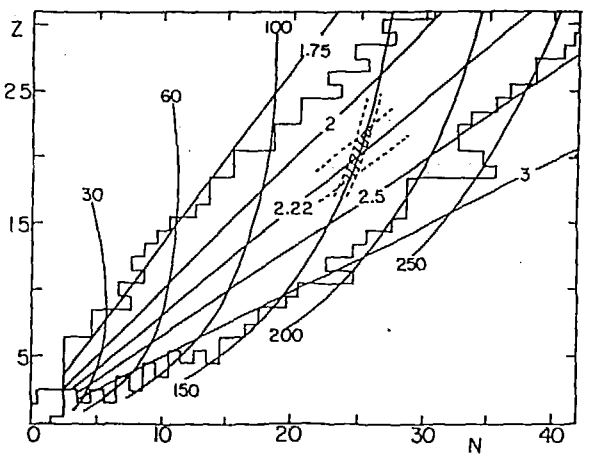

Fig. 3 : The two selections of the PFIS method in the (N,Z) plane

spectrometer are located in a (N, Z) domain such as represented by the lightly hatched area. This domain often includes only one isotope while in less favorable cases two or three are included.

III - 2 - Basis of the calculations

The characteristic properties of the PFIS method are derived from a few relations. The first one which plays a predominant role is a simple empirical relationship giving the range of a nucleus having an energy E :

$$(1)\quad R = K(A/Z^2)(E/A)^{\gamma}$$

In this expression K and γ are constants depending only on the stopping material. This relation was obtained by fitting the range-energy tables of Hubert et al. (3). The interest of this analytic expression is that it gives a simple formula to express the energy of the ion along its path in a stopping medium :

$$(2)\quad E_d/E = (1 - d/R)^{1/\gamma}$$

where E_d and E are the energies per nucleon of the (A, Z) ion at the depth d and at the entrance of the stopping medium respectively. The classical (non relativistic) relationship between the magnetic rigidity $B\rho$ and the mass, charge and energy per nucleon of the transmitted ion is the following :

$$(3)\quad B\rho = 0.1439\ (A/Z)\ \sqrt{E/A}$$

where $B\rho$ is exprimed in Tesla-meter. When combining equations 1 and 3 one may express the range as a function of A, Z and $B\rho$ only :

$$(4)\quad R = K'(1/r_2)(B\rho)^{2\gamma}$$

with $K' = K \times (0.1439)^{-2\gamma}$ and $r_2 = A^{2\gamma-1}/Z^{2\gamma-2}$

In the case of aluminium $\gamma \simeq 1.75$ and therefore $r_2 = A^{2.5}/Z^{1.5}$.

More complete studies are needed if one wishes to calculate the selection performances of the line, like the transmission yield and emittance of the selected fragments and the mass resolution. The target thickness, the shape and thickness of the degrader play crucial roles as we will see in the following. More details on the theoretical calculations concerning the PFIS method are fully described in Ref. 4.

III - 3 - Effect of the target thickness

Since the method is intended for exotic nuclei separation, one seeks to use a target as thick as possible to increase

the counting rate. An increase of the target thickness enlarges the energy distribution of the P.F. at the exit and may contribute to an increase of the mass acceptance. Consequently it is of prime importance to determine to which extent the increase in target thickness enhances the counting rate and not only contributes to an increase in the mass acceptance of the system.

In the target two processes broaden the energy spectrum of the P.F. :

i) the slowing-down process which gives different energy losses for the incident ion and the P.F.

ii) the nuclear reaction which induces an almost gaussian dispersion.

These two processes have a maximum effect for P.F. observed far away from the incident ion.

The effect of the target thickness on the mass acceptance of the first dipole is shown on Fig. 4. The calculations have been done for the study of ^{37}P in the fragmentation of an ^{40}Ar beam at 60 MeV/u in Al targets, the magnetic rigidity acceptance being 1.7%. In the case of a thick Al target (200 mg/cm^2) the transmitted ions are those inside the two outer boundary curves. For a thinner target the transmitted ions are those inside the two inner boundary curves. One can see that the thick target allows the transmission of ^{36}P and ^{38}P along with ^{37}P whereas only this last nuclide is transmitted in the thin target case.

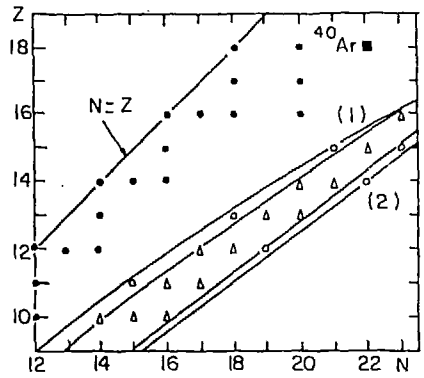

Fig. 4

A small part of the chart of the nuclides is represented. Full dots represent the stable isotopes, triangles represent the isotopes transmitted by the first dipole when an Al thin target (10mg/cm^2) is used, open dots designate the isotopes transmitted in addition to the triangles when a thick Al target (200mg/cm^2) is used.

The target thickness optimizing the transmitted yield of a given isotope is that which insures that all or part of the energy spectrum of this fragment falls in the Bp acceptance of the dipole. Detailed calculations about target thicknesses for P.F. having $r_1 = A/Z = 2.5$ like ^{37}P, lead to the curves represented in Fig. 5. The curve (1) gives the optimum target thicknesses as a function of the Z of the P.F. Two opposite evolutions are observed :

a) For the P.F. near the incident ion the optimum target thickness t_0 decreases with Z. This behavior is well understood as a combined effect of i) the slowing-down process in the target which enlarges the energy spectrum of light fragments for a given target thickness, ii) the acceptance of the dipole which limits the maximum acceptable target thickness.

b) For the P.F. far away from the incident ion, t_0 increases as Z decreases. But, in this case, t_0 does not represent the effective target i.e. the thickness used for the production of the transmitted ions. Indeed for these P.F. the nuclear energy spreading is so large that even for thin targets the momentum distribution cannot be fully accepted. The optimum target thickness represents the thickness giving the maximum effective target thickness t_e. In Fig. 5, the curve (2) represents the calculated t_e values as a function of the Z of the P.F.

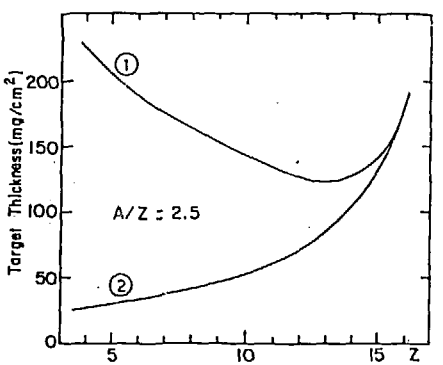

Fig. 5 : The target thickness is represented as a function of the Z of the P.F. for A/Z = 2.5. The curve (1) gives the optimum target thickness. The curve (2) gives the effective target thickness (see text).

The conclusions from this study are thus :

1) The target thickness optimizing the transmitted yield of a given $^{A}_{Z}$ isotope is function of A and Z.
2) The PFIS method has a maximum efficiency for the collection of fragments having A and Z close to that of the beam. This effect is superimposed on the cross section influence.

III - 4 - Effect of the intermediate degrader

After the first dipole, the selected ions undergo a slowing down in an Al degrader of thickness d located in the intermediate focal plane of the LISE spectrometer. The particules entering the degrader at the abscissa x (Ox being the horizontal axis in the focal plane and O the focal point) have a magnetic rigidity equal to :

$$(5)\quad B\rho_1(x) = B\rho_1\ (1 + x/D_1)$$

where D_1 is the dispersion of the first dipole exprimed in cm/% Bρ. After the degrader the value $B\rho_2(x)$ is given by the following relation deduced from Eqs. (2-3) of section III-2 :

$$B\rho_2(x)/B\rho_1(x) = \left(1-d(x)/R(x)\right)^{1/2\gamma}$$

The achromatism of the line is conserved if $B\rho_1(x)$ and $B\rho_2(x)$ are proportional for all x values. This is not true in most general cases. But if the shape d(x) of the degrader is such that d(x)/R(x) is independent of x the achromatism of the line is conserved. This condition is fulfilled with a wedge-shaped degrader of the following type (deduced from Eqs. 4-5) :

$$(6)\quad d(x) = d_0\ \left(1 + \frac{x}{D_1}\right)^{2\gamma}$$

This is a very simple formula where d_0 is a free scaling parameter equal to the degrader's thickness on the optical axis. D_1 and γ are characteristics of the LISE line and of the slowing-down process in the degrader's material respectively. The most striking result is that the wedge shape allowing to conserve the achromatism of the line is independent of the mass, charge and energy of the studied

ions as well as the tuning of the line. The practical realization of such a variable thickness is greatly eased if one achieves it by the bending of an homogeneous foil.

Let us now examine the influence of the intermediate degrader on the mass resolution and the image size in the focal plane of the second dipole. The minimum ΔA resolved is obtained when comparing the distance between the images of two isotopes $^{A}_{Z}$ and $^{A + \Delta A}_{Z}$ with the size of the image of the isotope $^{A}_{Z}$. In the simple case of an homogeneous degrader, an increase of the degrader thickness increases the diameter of the image while the mass resolution reaches only $A/\Delta A = 14$. A considerable improvement is obtained if the degrader is wedge-shaped in order to conserve the achromatism of the line. In this case the image size as well as the mass resolution is directly correlated to the ratio d_0/R of the degrader thickness d_0 to the range R of the A, Z nuclei at the exit of the first dipole. Using $d_0/R = 0.5$ (corresponding to $B\rho_2 = 0.8\ B\rho_1$), it is calculated that the image size increases of only a factor 2 whereas the mass resolution A/ΔA reaches 200.

As a conclusion of this paragraph, the preceding analysis gives a precise description of the most suitable geometry of the intermediate wedge-shaped degrader in order to conserve the achromatism of the line and to obtain the maximum mass resolution. Only an upper value of the resolution is obtained. This estimate indicates that the degrader's thickness must be at least half the total range of the ions at the exit of the first dipole when a mass resolution of 200 is desired.

IV - EXPERIMENTAL RESULTS

The PFIS method has been tested at LISE with an Ar beam at 60 MeV/u. As the slowing-down process in thick material is an essential part of the method, the used range-energy relations were first checked. A slight correction was then applied to better describe the experimental ranges.

IV - 1 - Experimental check of the PFIS method

The check of the magnetic rigidity determinations has been done with already known isotopes. In all cases the maximum counting rate was precisely observed for the "a priori" theoretical values. As an example the production of ^{30}Mg will be presented. This nucleus was unambiguously identified by mass spectrometry by Detraz et al (5). The γ spectrum observed in coincidence with the β decay of ^{30}Mg is shown in Fig. 6a. The $B\rho_1$ and $B\rho_2$

values were the theoretical ones calculated with a Be target thickness of 190 mg/cm^2 and an intermediate Al degrader of about 180 mg/cm^2.In this fig

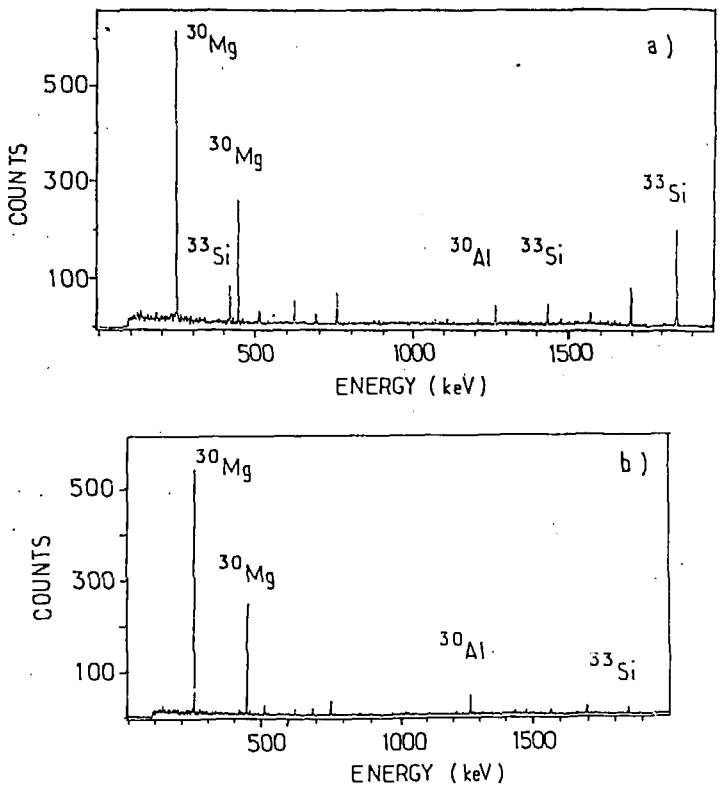

Fig. 6 : Two gamma spectra recorded for two different ($B\rho_1$, $B\rho_2$) tuning for the observation of ^{30}Mg

the 2 prominent peaks at 243 and 443 keV are those of ^{30}Mg. The decrease of these lines gives a half-life of (335 ± 40)ms in agreement with the previous determination (325 ± 30)ms. The line at 1263 keV belongs to ^{30}Al the daughter of ^{30}Mg. In this spectrum the contaminant is essentially ^{33}Si. The presence of this nucleus is understandable as ^{33}Si and ^{30}Mg have almost identical r_2 values and are thus not discriminated by $B\rho_2$. This contamination can be reduced by changing the magnetic rigidity of the first dipole. Indeed the r_1 value of ^{33}Si is only 5% lower than the r_1

value of ^{30}Mg. Using a $B\rho_1$ value 2% higher than the theoretical optimum value decreases the counting rate of ^{33}Si by more than a factor 10 whereas it decreases only by 20% for ^{30}Mg as it is shown in Fig. 6b.

The influence of the $B\rho_2$ tuning is much more critical than that of $B\rho_1$ if one wishes to transmit a given isotope. On Fig. 7 is plotted the evolution of the counting rate of ^{30}Mg as a function of $B\rho_2$ for a given $B\rho_1$ value. This curve allows us firstly to check the correspondance between the tuning parameters and secondly to get the experimental mass resolution in the focal plane. In this case the FWHM of the distribution in $B\rho_2$ is 0.9%. This corresponds to a total size of ∿ 2 cm in the focal plane and a mass resolution close to 100.

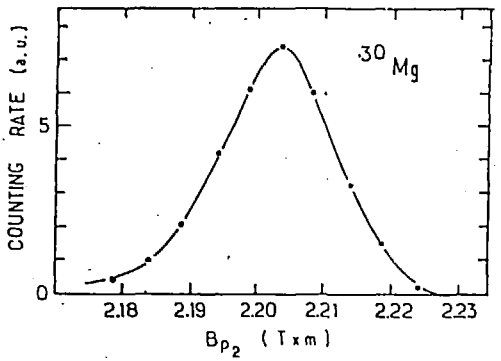

Fig. 7
The counting rate of the 243 keV γ-ray of ^{30}Mg is represented as a function of the tuning of the second dipole

IV-2 - New spectroscopic measurements

In the presented experiment, neutron rich nuclei have been produced and studied. The decay curve associated to each γ recorded in coincidence with β has been obtained as well as their precise energy and relative intensity. From these results, information on the decay scheme of the studied isotope and in some cases on the level scheme of its daughter are deduced.

This experiment is still under analysis and some results obtained up to now are given in Table 1. In this table the newly studied isotopes are listed together with the most prominent unambiguously detected γ rays. The measured half-life is given only when it represents a first measurement. The decay curves are presented in Fig. 8.

Isotope	Detected γ-ray energies (keV)	β-decay Half-life (s)
^{40}S	212 ± 2	7.6 ± 2.5
^{37}P	646 ± 1 752 ± 1 1582 ± 1	2.3 ± 0.2
^{38}P	1293 ± 1	.70 ± .15
^{35}Si	245 ± 1 395 ± 1	.80 ± .15
^{36}Si	175 ± 1	.40 ± .1
^{24}F	1982 ± 1	.33 ± .1
^{22}O	640 ± 1	

Table 1

β decay half-life of newly studied neutron rich isotopes and γ-ray energies detected in β-γ coincidence measurements.

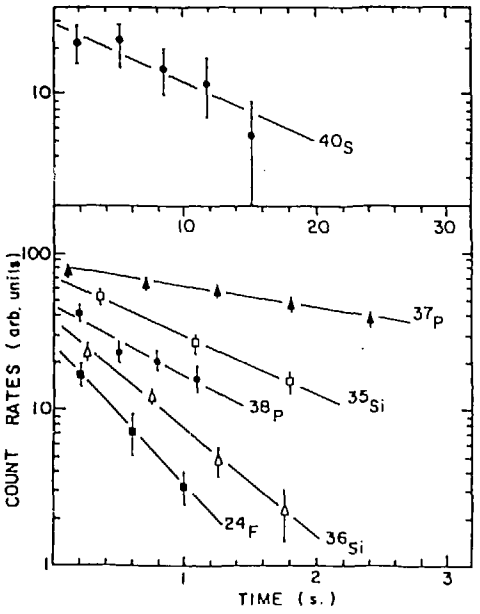

Fig. 8

The β-decay half-life data from this experiment along with their best fit curves

Comparisons between predictions and experiment for the half-life of nuclei lying far away from the stable ones provide good tests of the validity of the types of theoretical formulations and assumptions involved. The theoretical half-life predictions of Takahashi et al. (6), Klapor et al (7) and Wildenthal et al. (8) are compared to the measured ones in Fig. 9 for nuclei studied in this experiment as well as in refs. 9-12.

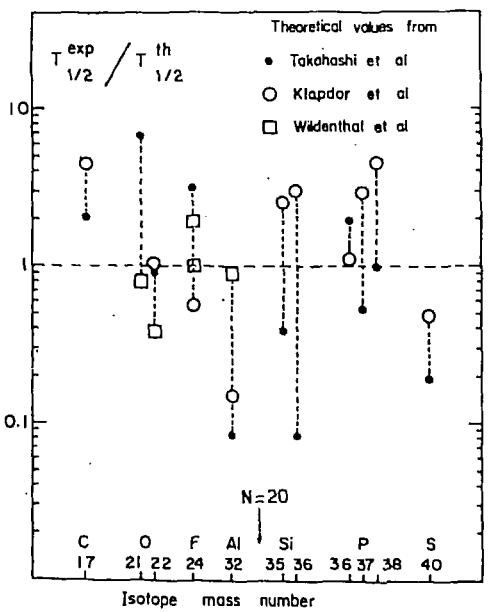

Fig. 9
Ratio of experimental and predicted β decay half-lives $T^{exp}_{1/2}/T^{th}_{1/2}$. The experimental values are from this work and refs. (9-12).

On the overall the measured half-lives lie between the calculated values. No systematic deviations are observed as it was the case in the Cr to Cu region (13). The mass domain presented in this fig. 9 covers the transitional region with the neutron shell closure at N = 20. One can notice that despite the fact that the microscopic calculations of Klapdor et al. certainly are improvements over the old gross theory of β decay, the reliability of such a model is still limited. With regards to the calculations of Wildenthal et al. for the sd nuclei, the agreement with experimental half-life values is quite good as there is only a factor 2 between the values in the less favorable cases.

Fig. 10 and 11 give examples of γ spectrum recorded in coincidence with the β decay of ^{36}P the last known isotope and ^{37}P.

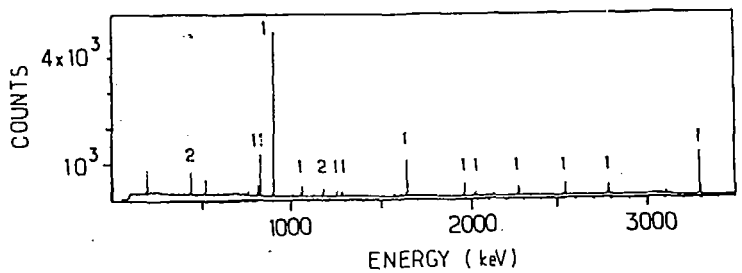

Fig. 10 : Gamma spectrum recorded in coincidence with the beta decay of ^{36}P.

In Fig. 10 peaks numbered (1) belong to ^{36}P, peaks numbered (2) belong to the contaminant ^{34}Si. The decay of ^{36}P to levels of ^{36}S was studied by Hill et al. (13). They only observed the three most prominent γ rays on this figure. Compared to the results of Hill et al. ten new lines are observed. A more complete decay scheme of ^{36}P and possible new ^{36}S levels are currently under analysis.

The γ spectrum recorded in coincidence with the β decay of ^{37}P is shown in Fig. 11. Three γ lines have been attributed to ^{37}P : γ_1 = (646.5 ± 0.5)keV, γ_2 = (752 ± 1)keV), γ_3 = (1585 ± 1)keV. The contaminant nuclei at the 1 to 5% level are ^{36}P and ^{39}S. The half-life

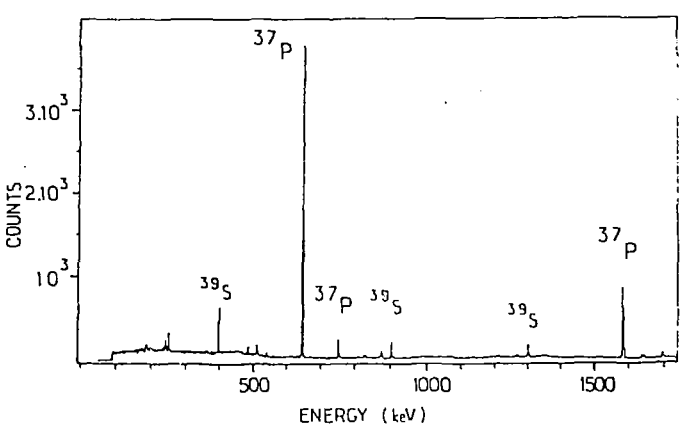

Fig. 11 : Gamma spectrum recorded in coincidence with the beta decay of ^{37}P.

was measured to be $T_{1/2}$ = 2.3 ± 0.2s for the three lines. The transitions γ_1 and γ_2 correspond to the feeding to the already known first excited states of ^{37}S. The transition γ_3 does not fit with the known levels of ^{37}S. The analysis of γ ray energies and intensities gives strong indication of a new ^{37}S level.

In the case of the β decay of ^{38}P one line has been unambiguously identified. This 1293 keV γ ray corresponds to the transition between the first known excited states of ^{38}S and the ground state. The measured half-life is (700 ± 150)ms.

Detailed β-γ spectroscopic studies on the nuclei presented in Table 1 will be published later.

V - CONCLUSION

The method exposed here allows us to use the LISE spectrometer as an isotopic separator by the adjunction of an intermediate energy degrader. This key part of the device has to be shaped in thickness in order to preserve the achromatism of the line. A striking result is that this condition is fulfilled for ions as different as ^{37}P and ^{15}C with the same shape of degrader. The theoretical mass resolution is close to 200 whereas the measured one reaches about 100. A neutron rich nuclei production experiment, still under analysis has been completed recently with an 60 MeV/u ^{40}Ar beam at GANIL. Several previously unknown half-lives have been obtained as well as β-γ spectroscopic information. These results demonstrate the possibilities of such a method. Future studies on the β decay of exotic nuclei are planned with heavier beams like Kr ions. In this case further improvements in the realization of the degrader are aimed at to provide a better mass resolution.

References

1 - D. Guerreau, Presented at the XXIII International Winter Meeting on Nuclear Physics (Bormio-January 1985) - Preprint GANIL P.85.02

2 - R. Anne and C. Signarbieux, GANIL Report RA/NJ 278/82 (1982) M. Langevin and R. Anne, Proc. Conf. on Instrumentation for Heavy Ion Nuclear Research, Oak Ridge, Tennessee, Oct. 22-24 (1984) ; GANIL Report 84-16 (1984)

3 - F. Hubert, A. Fleury, R. Bimbot and D. Gardès, Ann. Phys. France, 5S (1980) 1

4 - J.P. Dufour, R. Del Moral, H. Emmermann, F. Hubert, D. Jean, C. Poinot, M.S. Pravikoff, A. Fleury, H. Delagrange and K.H. Schmidt CENBG R.8536 - Le Haut Vigneau - F33170 GRADIGNAN-FRANCE - to be published in Nucl. Inst. Meth.

5 - C. Detraz, D. Guillemaud, G. Huber, R. Klapisch, M. Langevin, F. Naulin, C. Thibault, L.C. Carraz and F. Touchard, Phys. Rev. C19 (1979) 164

6 - K. Takahashi, M. Yamada, and T. Kondoh, At. Data & Nucl. Data Tables 12 (1973) 101

7 - H.V.Klapdor, J. Metzinger and T. Oda, At. Data & Nucl. Data Tables 31 (1984) 81

8 - B.H. Wildenthal, M.S. Curtin, and B.A. Brown, Phys. Rev. C28 (1983) 1343

9 - D.E. Alburger, C.J. Lister, J.W. Olness and D.J. Millener, Phys. Rev. C23 (1981) 2217

10 - M.J. Murphy, T.J.M. Symons, G.D. Westfall, and H.J. Crawford, Phys. Rev. Lett. 49 (1982) 455

11 - J.C. Hill, H.R. Koch, and K. Shizuma, Phys. Rev. C25 (1982) 3104

12 - M.S. Curtin, L.H. Harwood, J.A. Nolen, B. Sherill, Z.Q. Xie, and B.A. Brown, Phys. Rev. Lett. 56 (1986) 34

13 - V. Bosch, W.D. Schmidt-Ott, P. Tidemand-Petersson, E. Runte, W. Hillebrandt, M. Lechle, F.K. Thielemann, R. Kirchner, O. Klepper, E. Roeckl, K. Ryaczewski, D. Schardt, N. Kaffrell, M. Bernas, Ph. Dessagne, and W. Kurcewicz, Phys. Lett. 164B (1985) 22